Conversion of a Group II Intron into a New Multiple-Turnover Ribozyme That Selectively Cleaves Oligonucleotides: Elucidation of Reaction Mechanism and Structure/Function Relationships†

William J. Michels Jr.‡ and Anna Marie Pyle*,§

Department of Biochemistry and Molecular Biophysics and Integrated Program in Cellular, Molecular and Biophysical Studies, College of Physicians and Surgeons, Columbia University, New York, New York 10032

Received September 21, 1994; Revised Manuscript Received December 13, 1994⊗

ABSTRACT: The self-splicing ai5g group II intron was transformed into a three-part ribozyme that site-specifically cleaves small oligonucleotide substrates with multiple turnover. The ribozyme is composed of intron domain 1 (D1, 425 nucleotides), with catalytically essential domain 5 (D5, 58 nucleotides) provided separately as a reaction cofactor. Together, the D1/D5 complex cleaves small substrates analogous in sequence to the 5′-splice site of the intron. Activity of the ribozyme was studied using a combination of single- and multiple-turnover experiments in which the concentrations of the RNA components were varied in order to probe their individual role in the overall mechanism. Values for k_{cat}, K_m, and k_{cat}/K_m were the same within experimental error for the two enzymological approaches. These kinetic analyses reveal that the ribozyme utilizes a classic Michaelis−Menten reaction mechanism in which the chemical step of catalysis ($k_{cat} = k_{chem} = \sim 0.03$ min^{-1} at full saturation) is rate limiting for the overall reaction. The D1/D5 complex binds tightly to the substrate ($K_m = 6.3$ nM) and specifically recognizes sequences both 5′ and 3′ to the ribozyme cleavage site. These studies represent the first quantitative analysis of group II recognition and affinity for the 5′-splice site. As observed in previous studies on the role of D5 RNA, D5 binds tightly to the ternary complex ($K_m = 870$ nM). The second-order rate constant for RNA cleavage ($k_{cat}/K_m = 3.3 \times 10^6$) is an order of magnitude slower than that observed for other ribozymes in this mechanistic class, all of which are rate-limited by steps other than chemistry. That k_{cat} equals k_{chem} in this ribozyme is supported by the overall kinetic analysis and by the observation that an Rp phosphorothioate is cleaved ~3-fold more slowly than a phosphate at the cleavage site. These studies represent a preliminary examination of stereochemical preference by a group II intron active site in the transition state. The substrate specificity, reaction conditions, and mutational sensitivity of this ribozyme are consistent with a reaction analogous to the first step of group II intron self-splicing, although its stereochemical preference is analogous to a second-step reversal.

Self-splicing group II introns are essential for the processing of many organellar genes in plants and yeast (Michel et al., 1989; Kück et al., 1990). They have also been found to exist in prokaryotes (Ferat & Michel, 1993; Ferat et al., 1994). Group II introns are characterized by a conserved secondary structure that can be organized into six domains (Figure 1A) (Michel & Dujon, 1983). Of those six domains, domain 1 (D1)[1] and domain 5 (D5) have been found to be particularly important for catalytic function (Koch et al., 1992).

The splicing reaction is believed to be initiated by the 2′-hydroxyl group projecting from the bulged adenosine of domain 6 (D6), which attacks the 5′-splice site and generates a "lariat" intermediate (Peebles et al., 1986; Schmelzer & Schweyen, 1986; van der Veen et al., 1986). This step is followed by immediate attack of the 3′-hydroxyl of the 5′-exon on the phosphate at the 3′-splice site, resulting in ligated exons and lariat intron. Both steps of splicing can also proceed if the initial nucleophile is a water molecule rather than the 2′-OH of a bulged adenosine in D6 (van der Veen et al., 1987b; Jarrell et al., 1988b). There is little evidence that group II-dependent gene expression cannot proceed hydrolytically in vivo, as lariat species are accompanied by open molecules consisting of either broken lariats or hydrolytically generated species (Schmidt et al., 1987). In vitro self-splicing of the group IIA intron from *Podospora* proceeds predominantly through an apparent hydrolytic first step in vitro (Schmidt et al., 1990), and even for the group IIB intron ai5g, the hydrolytic pathway dominates under any reaction conditions that do not include molar quantities of ammonium ion (D. L. Daniels, W. J. Michels, and A. M. Pyle, manuscript in preparation). Hydrolysis also promotes the apparent first step of group II intron trans-splicing by 5′-exon-G oligonucleotides (Jacquier & Rosbash, 1986; Altura et al., 1989).

Domain 5 (D5) is the most phylogenetically conserved region of the group II intron, and it has been observed to act in-trans, promoting specific hydrolytic cleavage at the

† This work was supported by NIH Grants 1RO1GM50313-01 and T32DK07328 and the Irma T. Hirschl Fund for Medical Research.

* Author to whom correspondence should be addressed.

‡ Integrated Program in Cellular, Molecular and Biophysical Studies.

§ Department of Biochemistry and Molecular Biophysics.

⊗ Abstract published in *Advance ACS Abstracts,* February 1, 1995.

[1] Abbreviations: ai5g, the fifth intron of the gene for subunit I of yeast mitochondrial cytochrome oxidase; D1, domain 1 of the group II intron; D5, domain 5 of the group II intron; nt, nucleotide(s); E1a -19/8, substrate containing 19 nt of the 5′-exon and 8 nt of the ai5g intron; E1a -17/7, substrate containing 17 nt of the 5′-exon and 7 nt of the ai5g intron; E1E2 -19//-8, substrate consisting of ligated exon sequences flanking ai5g; PAGE, polyacrylamide gel electrophoresis; MOPS, 4-morpholinepropanesulfonic acid; EBS; exon binding site (on intron); IBS, intron binding site (on exon).

0006-2960/95/0434-2965$09.00/0

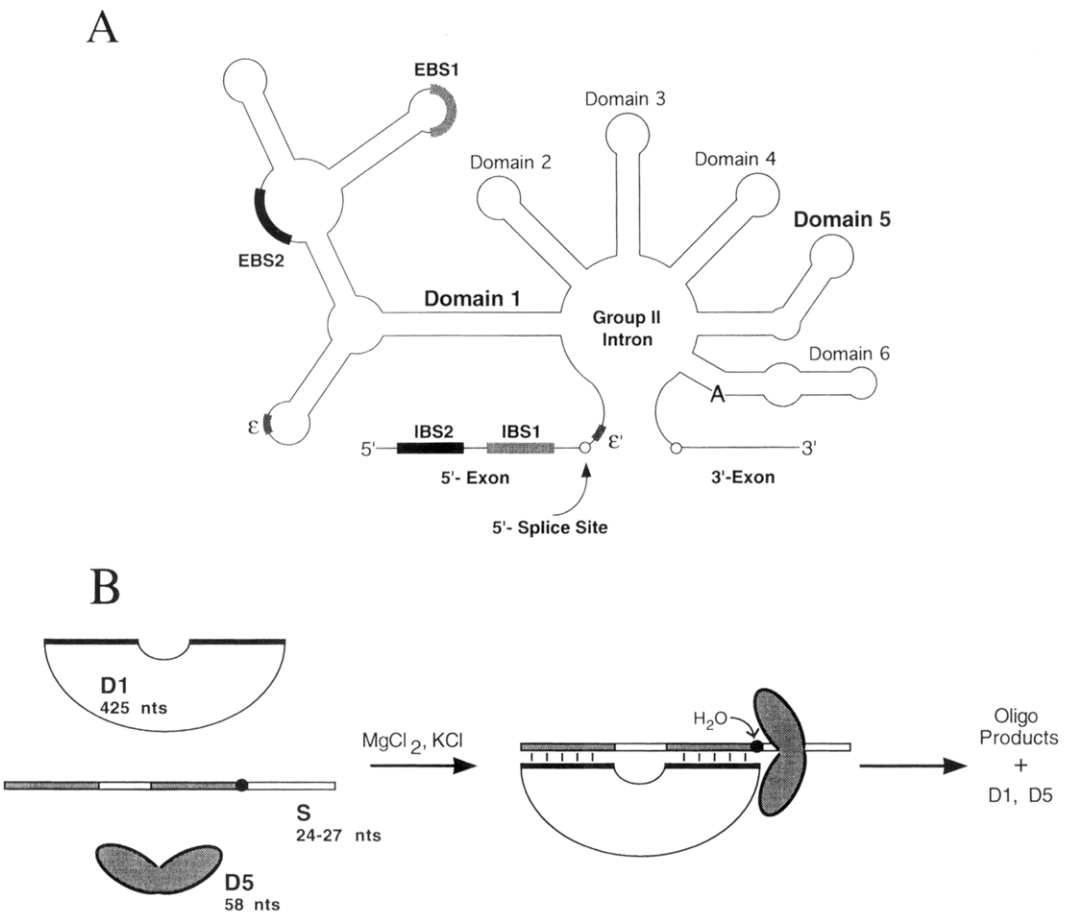

FIGURE 1: Schematic structures of a group II intron and the ribozyme derived from it. (A) Representative secondary structure of a group II intron. The EBS and IBS sequences are shown as bold or gray lines. Regions involved in the $\epsilon-\epsilon'$ interaction are shown as short bold lines. Although the ϵ region is shown at the end of a hairpin loop, there is actually a short stem projecting from this loop that is important for function (Suchy & Schmelzer, 1991). This schematic does not attempt to illustrate all the structural details found in group II introns, which are much more complex than indicated here. (B) Cleavage of a short RNA substrate (S) by the group II ribozyme. The domain 1 RNA molecule (D1) combines with a domain 5 (D5) RNA molecule and substrate (S) to catalyze specific cleavage at a site analogous to the 5′-splice site. Shaded regions and dashes between D1 and S designate pairing interactions IBS1•EBS1 (closest to the cleavage site) and IBS2•EBS2.

5′-splice site (Jarrell et al., 1988a). It is clear that D5 and D1 are absolutely required for the first step of splicing (Koch et al., 1992). Recent kinetic analyses have examined the hydrolysis of 5′-exon from domains 1−3 when D5 is provided in trans (Franzen et al., 1993; Pyle & Green, 1994). These studies showed that D5 associates with high affinity ($K_m \sim 300$ nM) to the other active site components. The strength of D5 binding is especially surprising considering that this small RNA (minimally ~40 nt) is largely duplex in form and, having no apparent phylogenetic covariation with the rest of the intron, seems to bind without the aid of base-pairing interactions. The D5-catalyzed reaction obeys a straightforward Michaelis−Menten mechanism in which the chemical step of hydrolysis appears to be rate-limiting (Pyle & Green, 1994).

Domain 1 of the group II intron is important for recognizing sequences on the 5′-exon. Analogous to the single internal guide sequence found in group I introns, D1 of group II introns contains a set of two exon binding sites (termed EBS1 and EBS2) that recognize complementary sequences immediately preceding the 5′-splice site (termed IBS1 and IBS2, Figure 1A) (Jacquier & Rosbash, 1986; Jacquier & Michel, 1987). These two base-pairing interactions (termed EBS1/IBS1, etc.) help to align the 5′-splice site within the catalytic core. While the pairing nearest the 5′-splice site (EBS1/IBS1) is generally believed to be the most important interaction (Muller et al., 1988; Wallasch et al., 1991), the additional EBS2/IBS2 pairing confers greater reactivity and reduces selection of cryptic splice sites (Muller et al., 1988). In addition to the EBS/IBS pairings, an additional short pairing known as the $\epsilon-\epsilon'$ interaction occurs between a region of D1 and intronic sequences immediately following the 5′-splice site (Jacquier & Michel, 1990). This interaction was shown to be important for both steps of splicing. Together, the EBS/IBS pairings and the $\epsilon-\epsilon'$ interactions (a total of approximately 20 nucleotides spanning the 5′-splice site) would seem to constitute the minimal site for recognition of the 5′-splice site by domain 1. However, deletion analyses of the exon sequences have indicated that additional exonic sequence as far as 52 nucleotides from the 5′-splice site may be necessary for efficient reaction (Jacquier & Rosbash, 1986; Jacquier & Michel, 1987; van der Veen et al., 1987a).

Group II introns, together with ribonuclease P (RNase P) and group I introns, form a class of catalytic RNAs that share a common overall mechanism of nucleophilic attack at phosphorus. These large RNAs fold into complex structures that are apparently necessary for carrying out several challenging catalytic tasks. In addition to binding an oligonucleotide and activating a specific phosphate residue for attack, RNAs in this family can also bind and activate

an exogenous nucleophile, orienting it precisely to carry out an S_N2 reaction on the activated phosphate group (Padgett et al., 1994). The leaving group in these reactions is always a 3′-hydroxyl, and the other product is a 5′-phosphate or a phosphodiester linkage. Because of their active-site complexity and the fact that there are only three known variations within this mechanistic class, each example is critically important to our understanding of RNA catalysis.

RNase P is a natural ribozyme, responsible for cleaving exogenous pre-tRNA substrates and generating mature tRNA molecules (Guerrier-Takada et al., 1983). Group I introns have been re-engineered from unimolecular self-splicing RNAs (Kruger et al., 1982) into multiple-turnover ribozymes, of which the *Tetrahymena* ribozyme is the best-studied example (Zaug & Cech, 1986). In both of these cases, (and in the case of small self-cleaving RNAs) a detailed understanding of the catalytic mechanisms of these RNAs was made possible by their construction as multiple-turnover enzymes (Zaug & Cech, 1986; Herschlag & Cech, 1990; Beebe & Fierke, 1994). With the RNAs in this form, the powerful techniques of mechanistic enzymology and biochemistry were readily applicable for the dissection of catalytic mechanism and active-site structure. One of the reasons that group II intron enzymology and folding remain poorly understood is that, until now, there were no analogous constructs of the group II intron which cleave oligonucleotides with multiple turnover.

In order to independently evaluate the role of D1, D5, and 5′-exon sequences on active-site folding and catalytic activity, we have constructed a modular group II intron ribozyme consisting of D1 (425 nt), which binds small oligonucleotide substrates (S, 24−27 nt) in trans. Efficient hydrolytic cleavage of this substrate at a single site is promoted by addition of a reaction cofactor (D5, 58 nts) that is also provided in trans (Figure 1B). This ribozyme is analogous to the *Tetrahymena* ribozyme (Zaug & Cech, 1986; Zaug et al., 1986) except that the cofactor is a short RNA which is unchanged in the reaction (Pyle & Green, 1994) instead of a nucleophilic guanosine that is consumed during reaction. With the reaction substrate and cofactors cleanly separated, it is now possible to hold any one component rate limiting in order to determine its precise role in binding or catalysis. The modular structure permits facile incorporation of mutations and single-atom changes for probing mechanism. We have used this ribozyme, which cleaves its substrate in an intermolecular fashion, to quantitatively characterize the association of the 5′-splice site with the catalytic apparatus and to determine individual rate constants along the reaction pathway. The reaction parameters generated by this analysis provide a kinetic framework for activity of a group II intron active site and facilitate intepretation of detailed structure−function relationships.

EXPERIMENTAL PROCEDURES

DNA Plasmids and Transcription Templates. Plasmid pT7D1 was constructed by PCR amplification of D1 from plasmid pJD20 (Jarrell et al., 1988a). Primers specifically amplified a 425-nt intronic fragment including all of D1, beginning with the +1G nucleotide of the intron. The upstream primer included a promoter for T7 RNA polymerase and a *Bam*HI restriction site. The downstream primer contained an *Eco*RI site. The PCR fragment was ligated into a pUC19 vector, expressed, and sequenced. Before transcription of D1 RNA, pT7D1 was linearized with *Eco*RI. D5 RNA was transcribed from plasmid pJDI5′-75 cut with *Hpa*II (Pyle & Green, 1994). Plasmids pJDI5′-75 and pJD20 were kindly provided by Dr. Philip S. Perlman. Synthetic DNA templates and top-strand oligonucleotides were used for transcription of substrate analogues (Milligan & Uhlenbeck, 1989). These were synthesized from phosphoramidites (Applied Biosystems, ABI) on an ABI 392 DNA/RNA synthesizer and then purified by PAGE.

RNA Transcriptions. D1 RNA (425 nt) and D5 RNA (58 nt) were transcribed under conditions described previously (Pyle & Green, 1994). The sequence of transcribed E1a -19/8 RNA substrates is 5′-GGAGUGGUGGGACAUU-UUCˇGAGCGGUU-3′ (where ˇ designates the ribozyme cleavage site). The all-phosphate substrate RNA (27 nt) was transcribed from a synthetic oligonucleotide template using the following modifications to published procedure (Milligan & Uhlenbeck, 1989): The concentrations of template and top-strand DNA were 0.3 μM each, and the NTP concentrations were 1 mM each. The transcription buffer contained 10 mM $MgCl_2$ (Aldrich, 99.99%), 100 mM KCl, 0.01% Triton X-100, 40 mM Tris, pH 8, 40 mM DTT, and 2 mM spermidine. The reaction mixture was incubated at 30 °C for 3−6 h. The substrate containing a phosphorothioate at the cleavage site was transcribed under the same conditions, with the following modifications: In place of GTP, there was 1 mM GMP and 1mM Sp α-thio-GTP (Amersham). GMP was added because priming of transcription by α-thio-GTP was inefficient for this oligonucleotide. These reaction conditions incorporate an Rp phosphorothioate linkage 5′ to every G residue in the substrate (Griffiths et al., 1987). This substrate was end-labeled with polynucleotide kinase and [γ-^{32}P]ATP. For use in a different experiment, a substrate containing phosphorothioates 5′ to each G residue and doped with ^{32}P 5′ to every C residue was transcribed according to the above conditions except that the reaction volume was smaller (~20 μL), the CTP concentration was 0.125 mM, and the [α-^{32}P]CTP concentration was 20 μM. All transcribed substrates were purified by 20% PAGE, which results in two major bands of equivalent intensity. Sequencing revealed that the lower of the two bands is the correct one, while the upper is the consequence of a common RNA-template directed T7 RNA polymerase side reaction (Cazenave & Uhlenbeck, 1994). After PAGE of all RNA transcripts, bands containing the desired RNA were cut from the gel and eluted into a buffer of 10 mM MOPS, pH 6.5, and 1 mM EDTA. RNA was recovered by ethanol precipitation. Concentrations were calculated spectrophotometrically from extinction coefficients determined as previously described (Pyle & Green, 1994).

Preparation of Synthetic RNA Substrates. Oligonucleotide substrate E1a -17/7 (5′-CGUGGUGGGACAUUUUCˇG-AGCGGU-3′) was chemically synthesized on an ABI 392 DNA/RNA synthesizer and deprotected according to standard procedures (Scaringe et al., 1990). Oligonucleotide tE1a -17/7, which contains a single phosphorothioate at the ribozyme cleavage site, was synthesized using tetraethylthiuram (TETD) as the sulfurizing oxidant for the CpG linkage at that site (Slim & Gait, 1991).

Reaction Conditions. All reactions were performed in 0.65-μL Slickseal tubes (National Scientific) using a final reaction volume of 20 μl. Before initiation of reaction, RNAs (in a 10 mM MOPS, pH 6.5, storage buffer) were mixed with water and buffer (80 mM MOPS, pH 7.5, final concentration at this point) in a total volume of 12 μL. This solution was then heated to 95 °C for 1 min to denature potentially misfolded RNAs formed during storage. After cooling to 42 °C, the reaction was initiated by adding 8 μL of concentrated salt mix to final reaction concentrations of of 100 mM $MgCl_2$ (99.99% pure, Aldrich), 1 M KCl, and 80 mM MOPS, pH 7.5. The validity of this procedure was checked by incubating the individual RNA components at 95 °C, adding salt mix to them individually, allowing them to incubate separately at 42 °C for varying lengths of time, and then initiating reaction by adding substrate to D1/D5 or in other combinations (see order of addition experiments). Reaction rates under these conditions were the same as rates obtained when reaction was initiated with salt mix. These control experiments, together with the absence of a lag in initial rates of all reactions, confirm the validity of the procedure. The use of ultrapure KCl (99.9999%, Aldrich) rather than reagent grade (99%) had no observable effects on the reaction. Aliquots of the reaction mixture were removed at indicated time intervals, combined with denaturing dye on ice, loaded on a 20% denaturing polyacrylamide gel (PAGE), and quantitated on a Betagen Betascope or Packard Instant Imager using methods previously described (Pyle & Green, 1994).

Single-Turnover Kinetics. In these enzyme excess experiments, reactions were performed using trace concentrations of 5′-^{32}P-end-labeled substrate RNA (0.5 nM unless indicated) and excess concentrations of D1 and D5 RNAs (as the enzyme and cofactor, respectively). Reaction rates (k_{obs}) were determined by plotting the natural logarithm of the fraction of substrate remaining vs time and solving the equation of the line for reaction half-time [$t_{1/2} = (\ln 2)/ k_{obs}$]. Values of k_{obs} at saturation did not vary from 0.01 to 3 nM [S], indicating that pseudo-first-order kinetics apply. Pseudo-first-order semilog plots of the cleavage time course were linear for >3 reaction half-times. Early time points (generally <50% completion) were used in the calculation of k_{obs}. Individual values of k_{obs} determined over a 6-week time period with the same RNA stocks varied by 18% (with 95% confidence and five trials).

Multiple-Turnover Kinetics. In these substrate excess experiments, D1 was present in trace concentrations (0.5 nM, as the enzyme), D5 was saturating (3 μM, as the cofactor), and S was in excess over D1. Plots of [P] vs time were used to obtain reaction rates at eight different substrate concentrations (2−50 nM). Plots were linear for at least 16 turnovers (the maximum we examined), although precise rates were calculated from data obtained early in the reaction (from <1 to 3 turnovers, depending on the [S]). Individual values of k_{obs} at a single concentration of S varied by 19% (based on three trials, with 95% confidence limits). Values of k_{obs} were plotted in an Eadie−Hofstee format to generate the steady-state kinetic parameters K_m, k_{cat}, and k_{cat}/K_m. This entire experiment was conducted twice, yielding no single kinetic parameter that differed by more than 50% between experiments.

Nuclease Digestions. For sequencing the transcribed oligonucleotides, enzymatic digestions with endonucleases U2, *B. cereus*, T1 (Pharmacia), CL3 (Boehringer), and hydroxide were carried out under standard conditions (Donis-Keller et al., 1977). Partial P1 nuclease digests were performed using 50 mM sodium acetate buffer, pH 5.3, 0.05 μg/μL tRNA, and 5 × 10^{-6} units/μL P1 nuclease (Boehringer) for 30 min at 37 °C. For experiments designed to determine whether transcribed phosphorothioate linkages were cut to completion by the ribozyme, RNA substrates were ethanol precipitated after treatment with ribozyme (or with equivalent an amount of carrier tRNA) and then treated with P1 nuclease (Potter et al., 1983). P1 nuclease digestion of the transcribed all-phosphate and phosphorothioate substrates was performed under the following conditions: RNA (3000 cpm) was incubated with 0.01 unit/μL P1 nuclease in 25 mM acetate buffer, pH 5.3, 10 mM DTT, and 0.05 μg/μL tRNA competitor for 30 min at 37 °C.

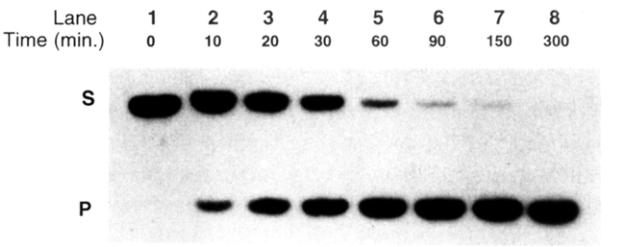

FIGURE 2: A time course of oligonucleotide cleavage by the ribozyme. Ribozyme cleavage of transcribed substrate (S) 5′-^{32}P-GGAGUGGUGGGACAUUUUC˘GAGCGGUU-3′ to a 5′-end-labeled 19-nt product (P) and an 8-nt unlabeled product; the cleavage site is marked with a "˘" and IBS sequences are underlined. Lanes 1−8 correspond to a reaction of S (1 nM) in the presence of saturating D1 (100 nM) and D5 (3 μM). The reaction was performed under standard reaction conditions (42 °C in 80 mM MOPS (pH 7.5), 1 M KCl, and 100 mM $MgCl_2$).

RESULTS

Cleavage of Oligonucleotides by the Ribozyme. The self-splicing ai5g group II intron was transformed into a two-piece ribozyme consisting of separate D1 and D5 subunits. This ribozyme assembly cleaves small oligonucleotides containing the sequence analogous to the 5′-exon/intron boundary of the ai5g group II intron (Figure 1B). In the presence of saturating concentrations of D1 and D5 (determined initially by spot-checking the rate effects of increasing [D1] and [D5]), a substrate oligonucleotide is readily cleaved to completion (Figure 2) specifically at the CpG sequence that corresponds to the normal 5′-splice site. If either D1 or D5 is absent from the reaction, substrate is not cleaved. Previous studies showed that a minimum exon length of 52 nt (terminating in the CpG cleavage site) was required for trans-splicing or trans-cleavage by the ai5g group II intron (Jacquier & Rosbash, 1986; Jacquier & Michel, 1987). In our study 17 nt of exon, encompassing both IBS1 and IBS2, was sufficient for efficient cleavage. However, the substrate used in this study also contains 7−8 nucleotides of intronic sequence, including nucleotides (+3 and +4) involved in the $\epsilon-\epsilon'$ interaction believed to stabilize 5′-splice-site association (Jacquier & Michel, 1990).

Kinetic Parameters from Single-Turnover Analyses. These experiments were conducted using trace amounts of substrate such that [S] ≪ K_m. The kinetic parameters as a function of limiting [D1] (K_m^{D1} and k_{cat}/K_m^{D1}) were evaluated by holding [D5] at saturation and varying the concentration of

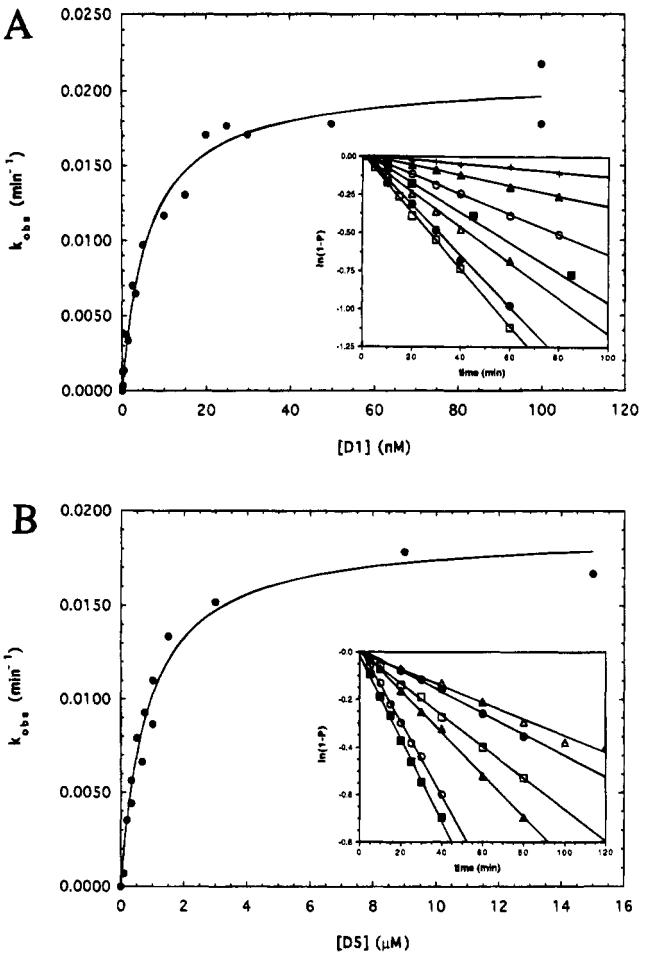

FIGURE 3: Single-turnover kinetics of oligonucleotide cleavage by the three-part group II ribozyme. A synthetic oligonucleotide substrate (S) was cleaved under varying conditions of excess [D1] and [D5] in order to resolve individual kinetic parameters. The sequence of this oligonucleotide is 5′-CGUGGUGGGACAU-UUUC˜GAGCGGU-3′. (**A**) Inset: Representative pseudo-first-order plots for cleavage of S (0.05 nM) at saturating D5 (3 μM) and varying concentrations of D1 (0.5, 1.5, 3.25, 5, 10, 20, and 100 nM shown). Hyperbolic plot: The k_{obs} values determined from the inset plots were graphed against [D1] to generate the apparent binding curve for D1. (**B**) Inset: Repesentative pseudo-first-order plots for cleavage of S (0.1 nM) at saturating D1 (25 nM) and varying amounts of D5 (0.2, 0.33, 0.67, 1, 3, and 9 μM shown). Hyperbolic plot: The k_{obs} values determined from the inset plots were graphed against [D5] to generate the apparent binding curve for D5 and the kinetic parameters shown in Table 1 (line 3). In the hyperbolic plots in both (A) and (B), the k_{cat} value for the reaction is the horizontal asymptote of plots ($\sim$ 0.02 min^{-1}), and K_m is the concentration of enzymatic subunit at which $k_{obs} = 0.5k_{cat}$. Values of k_{cat} and K_m were determined from the fit of the curves shown to an equation describing 1:1 bimolecular association (Pyle & Green, 1994). The kinetic parameters and standard error for the fit are provided in Table 1 (line 1). The appropriateness of the standard error calculation was confirmed using a jackknife approximation of standard error (Pyle & Green, 1994).

D1 from below to above its K_m with the ternary complex (Figure 3A). The parameters as a function of limiting [D5] (K_m^{D5} and k_{cat}/K_m^{D5}) were evaluated in a corresponding manner (Figure 3B). The synthetic 24-nt substrate used in these studies had an empirically determined endpoint of 82% reacted after >7 reaction half-times. This value was used to correct the data presented in the pseudo-first-order plots (Figure 3, insets). The transcribed 27-nt substrate had an end point of 96% after >7 reaction half-times.

For conditions under which [D1] was rate-limiting, kinetic parameters were determined by monitoring the cleavage rate of trace [S] in the presence of saturating D5 through a range of D1 concentrations (Figure 3A; Table 1, line 1). In this case, each D1 was expected to be associated with D5, and overall rate was limited by the concentration of this D1·D5 complex. The resulting curve of k_{obs} values as a function of D1 would therefore reflect the affinity of the ternary complex for the substrate RNA. The good fit of the rate data to a bimolecular binding isotherm provides strong support for this model. The K_m^{D1} determined from Figure 3A is 6.3 nM, implicating strong association between S and D1. This is the first quantitative assessment of affinity between 5′-splice-site sequences and D1. At very high concentrations of D1 (the plateau of the plot in Figure 3A), S is completely saturated with both components of the ternary complex and k_{obs} reflects the conversion of E·S $\rightarrow$ E·P, where E represents D1 that is fully saturated with D5 cofactor and P represents reaction products. Under these saturating, single-turnover conditions, the apparent rate (defined here as k_{cat}) represents the rate of the chemical step and any conformational changes that take place within the E·S complex. The k_{cat} value at saturating [D1] was 0.021 min^{-1}.

For conditions under which [D5] was rate-limiting, values for K_m^{D5}, k_{cat}^{D5}, and k_{cat}/K_m^{D5} were determined by monitoring the cleavage rate of S in the presence of saturating D1 through a range of D5 concentrations (Figure 3B; Table 1, line 3). In this case, each molecule of S was bound to D1 and overall rate was limited by the concentration of D5. The K_m^{D5} is 870 nM, k_{cat}/K_m^{D5} is 2.2 $\times$ 10^4 M^{-1} min^{-1}, and k_{cat} is 0.019 min^{-1}. Values of k_{cat} from both D1- and D5-limited experiments are in close agreement (Table 1).

In order to conserve D5 RNA, the single-turnover experiments in which D1 was varied were all conducted at 3 μM D5 (Figure 3A). This value is slightly below total saturation if K_m is 870 nM. Conversely, the experiments in which D5 was varied were all conducted at a [D1] that was slightly below saturation (25 nM; Figure 3B). This was done to ensure that at low [D5], the [D5] always remained higher than the [D1]. This design limited the possibility for a free D1 to bind S and create a potentially dead-end complex, although no such species has been observed. The amount by which D5 and D1 were below saturation was readily extrapolated from the hyperbolic plots shown in Figure 3. Theoretical k_{cat} values at ∞D1 and ∞D5 were then calculated, and both were found to be in agreement with a value of 0.026 min^{-1}, determined experimentally at 100 nM D1 and 9 μM D5.

Kinetic Parameters from Multiple-Turnover Analysis. Depite the fact that the D1 and D5 subunits combine to cleave small RNAs, they are not behaving enzymatically unless they can cleave substrate with multiple turnover. In addition, a steady-state kinetic analysis can provide valuable insight into the reaction mechanism. For these reasons, we conducted a kinetic analysis of the ribozyme under multiple-turnover reaction conditions (Figure 4). In these experiments, the enzyme (D1, saturated with D5) was present at trace concentrations and the substrate RNA was in large excess. Because the concentration of enzyme in these reactions is so low, this experiment is very sensitive to the presence of improperly folded or defective pools of the D1 RNA. Nonetheless, a reciprocal plot of reaction rate vs [S] reveals kinetic parameters remarkably close to those observed

Table 1: Kinetic Parameters for Substrate Cleavage by the Group II Ribozyme:

substrate	kinetic approach[a]	k_{cat} (min^{-1})[b]	K_m (nM)[b]	k_{cat}/K_m (M^{-1} min^{-1})[c]	k_{obs} thioS (min^{-1})[d]	thio-effect[e] on k_{cat}
E1a-17/7	ST (D1)	0.021 ± 0.0038	6.3 ± 0.88	(3.3 ± 0.76) × 10^6	0.012	1.8
E1a-17/7	MT	0.020 ± 0.0057	9.2 ± 4.1	(2.2 ± 1.1) × 10^6		
E1a-17/7	ST (D5)	0.019 ± 0.0034	870 ± 110	(2.2 ± 0.62) × 10^4		
E1a-19/8	ST	0.032+ 0.0048			0.0094	3.4

[a] Single-turnover (ST) or multiple-turnover (MT) kinetic analyses where the concentration of one component held was rate-limiting (in parentheses). For ST experiments, the component listed (either D1 or D5) was rate-limiting, while the unlisted enzyme component was at saturation. For the E1a-19/8 substrate, both D1 and D5 were fully saturating. For MT experiments, D1 was present in trace amounts, D5 was saturating, and S was in excess over D1. [b] k_{cat} and K_m represent the maximum rate and apparent binding constants under the indicated conditions described in Figure 3 (for lines 1 and 3), in Figure 4 (line 2), and in the text. Only k_{cat} is provided for substrate E1a-19/8. It represents the k_{obs} at D1 and D5 saturation for cleavage of a transcribed all-phosphate substrate at full saturation of both D1 and D5. The error in single-turnover k_{cat} values is most conservatively provided as the variance for a single k_{obs} (18%, with 95% confidence after 5 trials). Standard errors are much lower. The error in single-turnover K_m values is the standard error calculated as described (caption, Figure 3). The variance in multiple-turnover data was calculated using a least squares fit of the data to the line of an Eadie–Hofstee plot (Figure 4). [c] k_{cat}/K_m values were determined by dividing k_{cat} by K_m. They are consistent with k_{cat}/K_m values determined from the slopes of k_{obs} vs [D1] or [D5] at very low concentrations in ST experiments. Reported error was propagated from the k_{cat} and K_m standard errors. [d] The reported rates represent k_{obs} values for phosphorothioate substrates at saturation, where [D1] = 100 nM and [D5] = 3 μM as in Figure 2. Each value is the average of two trials. Like all reported k_{obs}, maximum variance is 18%. The empirically determined endpoints (after >7 reaction half-times) used in calculation of k_{obs} was 82% for the transcribed phosphorothioate substrate and 48% for the synthetic phosphorothioate substrate. [e] The ratio of k_{cat} (phosphate) to k_{obs} (phosphorothioate) for substrates at saturation.

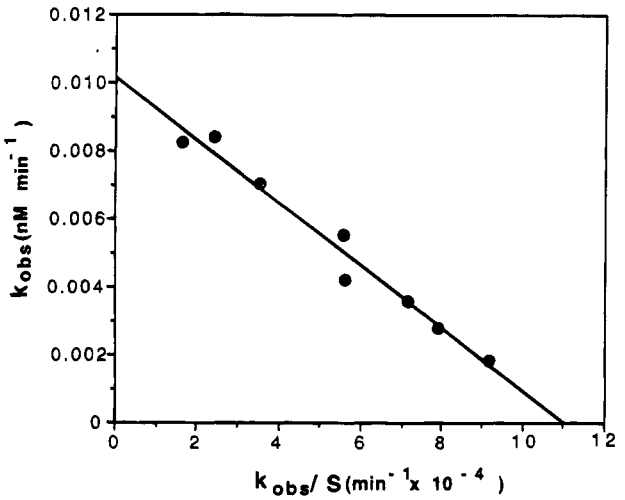

FIGURE 4: Eadie–Hofstee plot of multiple-turnover kinetics. The apparent rates of multiple-turnover reactions (k_{obs}) were plotted vs k_{obs}/[S], where [S] is expressed in nM. The enzyme (D1) concentration used in these experiments was 0.5 nM. The equation of the line for the Eadie–Hofstee plot shown is $y = -9.2x + 0.010$, resulting in the kinetic constants shown in Table 1 (line 2). The slope of the line is equal to $-K_m$, and the y-axis is equal to V_{max} ($k_{cat} = V_{max}/[D1]$). A linear regression was used to compute standard errors in the kinetic parameters (Table 1). Individual k_{obs} values in the multiple-turnover analysis were found to vary by ±19% for experiments done on different days (using three trials and a 95% confidence limit).

for the parallel single-turnover reactions in which the [D1] was held rate-limiting and D5 was at saturation (K_m^{D1} and k_{cat}/K_m^{D1}) (Figure 3A). The value for k_{cat} under multiple-turnover conditions (0.020 min^{-1}; Table 1 line 2) closely matches that of single-turnover conditions. The D1 enzyme readily turns over, cleaving many rounds of substrate. Previous work on the 5′-splice site hydrolysis of a cis-5′-exon has already shown that D5 RNA can turn over and cleave many rounds of exon 1/domains 1–3 RNA (Pyle & Green, 1994; Franzen et al., 1993). The resulting kinetic parameters are similar to the single-turnover parameters shown here for reactions in which [D5] is held rate-limiting (Table 1, line 3) (Pyle & Green, 1994).

Order of RNA Addition Experiments. We attempted to determine whether formation of the active ternary complex depends on simultaneous addition of particular reaction components. For example, domain 1 may not be able to fold properly unless substrate is present. To address this issue, two of the three RNAs were incubated for 60 min under standard reaction conditions. Reaction was then initiated by addition of the third RNA component such that the final RNA concentrations were 0.5 nM D1, 3 μM D5, and 3.5 nM S. Three parallel reactions were carried out in which the third RNA was different in each case. Product evolution vs early reaction time was monitored for less than 1 turnover. For the three reactions, k_{obs} differed by less than 1% and the linear plots of [P] vs time were superimposable. The second-order rate constants determined from these plots correspond to data shown in Table 1 (line 2, derived from Figure 4), from experiments in which all reaction components were added simultaneously. Taken together, these observations indicate that there is no preferred pathway of addition for the reaction components and that, within the time scale of this reaction (measurable accurately within a few minutes), the RNA components D1 and D5 act as independent folding domains. It is important to note that analogous experiments were done under enzyme excess conditions and there were no rate effects observed for any pairwise preincubation of RNA components in reaction buffer.

Substrate Mutations That Reflect the First Step of Splicing. In group II introns, mutation of the +1G at the 5′-splice site results in large rate effects that are specific to the first step of splicing. While +1A and +1U mutations have small effects, +1C substitution radically inhibits the first step of splicing (Chanfreau & Jacquier, 1993; Peebles et al., 1993). In order to determine whether ribozyme activity reflects a reaction analogous to the first step of splicing, we conducted parallel, single-turnover kinetic analyses on transcribed substrates containing mutations at the +1 position, together with wild-type and ligated exon substrates (Table 2). The data reveal that +1C mutation reduces cleavage efficiency by 20-fold, while +1A and +1U mutations have minimal effects. This behavior is consistent with a reaction analogous to the first step of splicing. The dramatic rate decrease seen in ribozyme cleavage of a substrate consisting of spliced (ligated) exons (Table 2) is inconsistent with a reaction analogous to a second-step reversal or "spliced-exon reopening" reaction.

Table 2: Kinetic Effects of Base Changes at the Ribozyme Cleavage Site

substrate[a]	k_{obs} (min^{-1})[b]	rel rate
+1G (WT)	0.036[c]	1.0
+1A	0.053[c]	1.5
+1U	0.028[c]	0.79
+1C	0.0019[d]	0.05
ligated exons	0.0068[d]	0.19

[a] The sequence of transcribed substrates used to monitor mutational effects at the 5′-splice site is 5′-GGUGUGGUGGGACAUUUUC-ˇNAGCGGUU, where N marks the +1 nucleotide at the cleavage site. The sequence of the ligated exons substrate is 5′-GGAGUGGUGG-GACAUUUUCˇACUAUGUA, where the underlined nucleotides are 3′-exon sequences. Rates are not affected by identity of the first three 5′-nucleotides. [b] All rates were obtained simultaneously, so it is expected that their relative error is very low (<5%). The absolute error for k_{obs} values reported in this study is ±19% with 95% confidence (see the footnotes to Table 1). [c] Pseudo-first-order plots were linear for at least four reaction half-times (as in Figure 7), and empirically determined endpoints of 92−94% were used for data correction. [d] For these slower substrates, evaluated at <20% reaction extent, a 92% endpoint was used in calculations of k_{obs}.

Cleavage and Mapping of Transcribed Phosphate and Rp Phosphorothioate Substrates. In order to determine whether the ribozyme cleaves an Rp phosphorothioate diastereomer, a new substrate was prepared by in vitro transcription. T7 RNA polymerase incorporates only Rp phosphorothioates into RNA polymers (Griffiths et al., 1987). Using α-Sp-thio-GTP, we transcribed an RNA substrate containing an Rp phosphorothioate at every G residue, including the 5′-splice site (5′SS). Just as the ribozyme specifically cleaves a phosphodiester linkage at the 5′SS sequence (Figure 5, lane A8), the ribozyme specifically cleaves a substrate containing an Rp phosphorothioate linkage at the cleavage site (Figure 5, lane B8). To confirm that the ribozyme cleaves both phosphodiester and phosphorothioate RNA substrates uniquely at the 5′SS sequence, the transcribed substrates and products were mapped with a battery of sequence- and stereospecific nucleases (Figure 5, lanes 4−7 and 9). The substrate containing all-phosphate linkages was mapped next to the substrate containing phosphorothioates at G residues (Figure 5, sections A and B). The proper sequence at the cleavage sites was confirmed by digestion of substrates with CL3 (Boguski et al., 1979), *B. cereus*, and T1 endonucleases (Donis-Keller et al., 1977). Product oligonucleotides migrate at the expected position relative to specific nuclease cuts at −1C and +1G on the substrates. The endonucleolytic digests described above, together with U2 digestion, confirmed the absolute sequence throughout both substrates (Figure 5). The migration of the ribose product with a 19-mer P1 endonuclease digestion product suggests that the group II ribozyme leaves 3′-OH and 5′-phosphate termini. The presence of a phosphorothioate at the cleavage site was confirmed by a gap in the P1 nuclease ladder of the thio substrate (Figure 5, lane 9) (Potter et al., 1983), together with I_2 cleavage of the thio substrate (I_2 data not shown) (Schatz et al., 1991). Taken together, these data indicate that the ribozyme is selecting the proper cleavage site on both phosphate- and phosphorothioate-containing substrates. Thus, the ribozyme readily cleaves the Rp diastereomer of a transcribed substrate and does not select adjacent phosphate sites for attack.

Even though the ribozyme specifically cleaves a transcribed substrate at an Rp phosphorothioate, the partial digests do not provide quantitative evidence that the substrate sequence and linkage sulfur content are homogeneous at that site. Significant dethioation at the splice-site linkage would result in conversion to phosphate and apparently efficient cleavage by the ribozyme. We also sought a quantitative demonstration that the group II ribozyme cleaves a linkage that is uncleavable by P1 endonuclease, which prefers to attack Sp phosphorothioates. In addition to proving that the ribozyme could cleave a homogeneous Rp linkage, we wanted to unambiguously demonstrate that the site of ribozyme cleavage is the CpG linkage at the 5′-splice site target sequence. To this end, a thio substrate was transcribed in the presence of [α-^{32}P]CTP. Because P1 endonuclease cannot cleave Rp phosphorothioates, a total P1 digest of this substrate leads to three products in approximately equimolar ratios: *pC, *pCp_sG, and *pCp_sGp_sG, where p_s indicates a phosphorothioate linkage (Figure 6, lane 3). Because the intensities of the three bands are approximately equal, this indicates that the substrate has been faithfully transcribed by T7 RNA polymerase and that the cleavage site dinucleotide must be an Rp phosphorothioate linkage. When a sample of internally ^{32}P-labeled substrate is cleaved to completion by the ribozyme and then immediately digested with P1 under similar conditions, two predominant bands are observed: *pC and *pCp_sGp_sG (Figure 6, lane 4). The middle p*Cp_sG band, corresponding to the ribozyme cleavage site, is considerably diminished in intensity, while the *pC band is correspondingly enhanced. Incubation of substrate with D1 or D5 alone followed by P1 digestion does not result in a diminution of the middle p*Cp_sG band (Figure 6, lanes 5 and 6). These results quantitatively demonstrate that this group II ribozyme specifically cleaves a CpG linkage that is uniformly Rp phosphorothioate in identity.

Determination of a Rate-Limiting Chemical Step. A synthetic oligonucleotide substrate was synthesized containing a single phosphorothioate linkage at the ribozyme cleavage site. Synthetic phosphorothioate linkages theoretically contain an equimolar mixture of Rp and Sp phosphorothioate diastereomers. When this diastereomeric mixture was reacted with the ribozyme under standard conditions at saturating concentrations of D1 and D5, only 50% of the substrate was cleaved. Like many enzymes, the ribozyme is presumed to prefer one of the two diastereomers. Taking into account the 50% endpoint for cleavage of the synthetic substrate, a rate constant for cleavage of the preferred phosphorothioate diastereomer was readily obtained (Table 1). A 2-fold diminution in rate (the "thio effect") was observed for cleavage of a phosphorothioate linkage. The transcribed substrate containing an Rp phosphorothioate linkage at the reaction site was cleaved with a k_{cat} value approximately 3-fold slower than that of a transcribed, all-phosphate substrate (Figure 7). Like the thio effect observed by using synthetic substrates, this value is consistent with an apparent rate-limiting chemical step (Table 1, column 7). The rate of cleavage in the transcribed Rp case is the same (within error) as that of the 50% synthetic substrate that is cleavable by the ribozyme (Table 1). Therefore, phosphorothioates at positions other than the cleavage site on the transcribed substrate have little apparent effect on rate. For phosphate and phosphorothioate substrates, measurement of k_{obs} was confirmed to be under saturating conditions because rate did not change appreciably with increased [D1] and [D5]. The thio effect itself was unchanged by increasing concen-

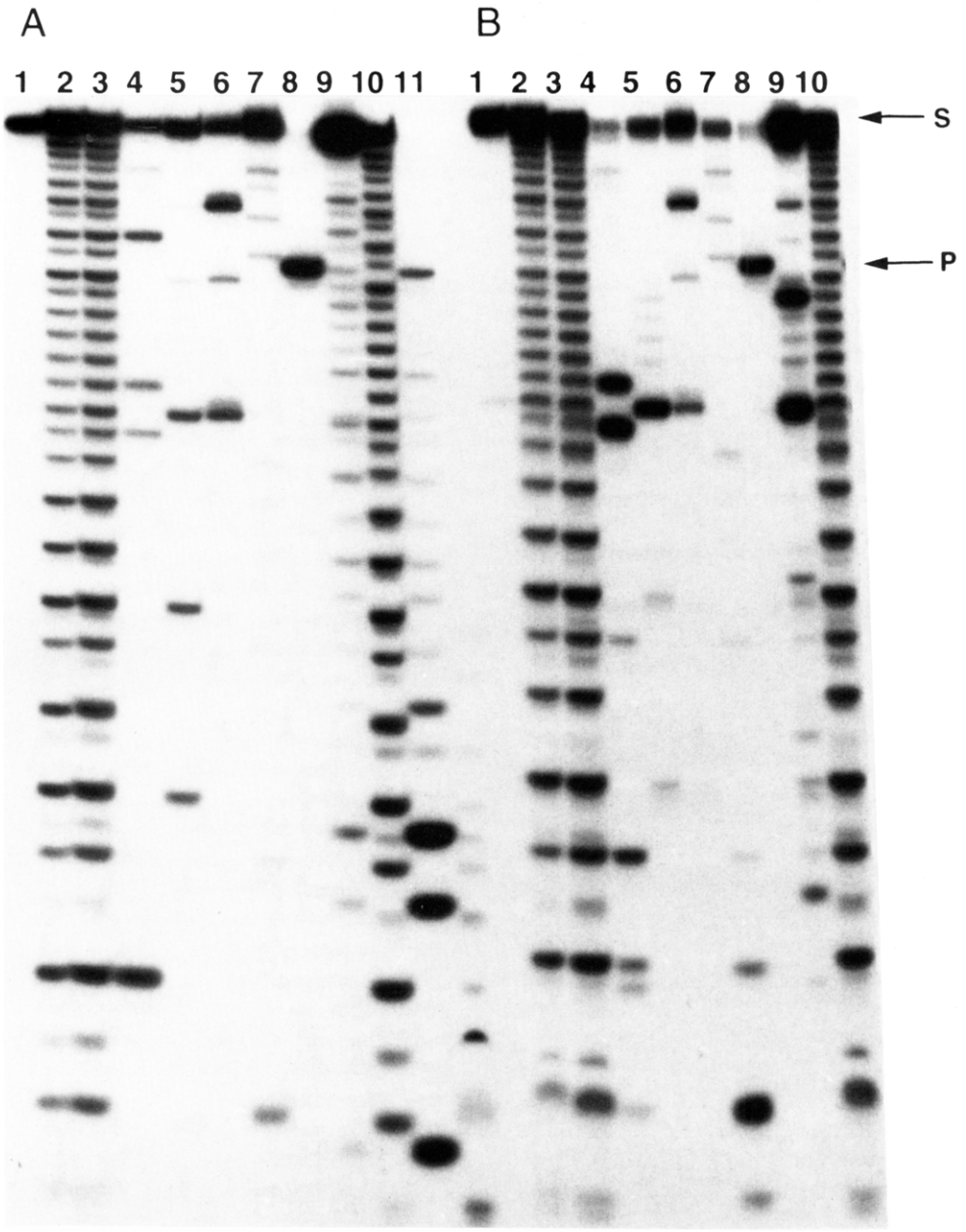

FIGURE 5: Nuclease mapping of transcribed substrates and their cleavage products. Panel A: Nuclease digestions of [5′-^{32}P]E1a -19/8 (transcribed all-phosphate substrate). Panel B: parallel nuclease digestions of [5′-^{32}P tE1a -19/8 (transcribed from the same template as E1a -19/8, but using α-thio Sp GTP as the sole source of GTP in the reaction). S and P (at right) signify mobilities of substrate and product, respectively. Oligonucleotide tE1a -19/8 contains an Rp phosphorothioate residue 5′ to every G, including the cleavage site. For both panels A and B, lane 1 is the full-length substrate; lanes 2 and 3 are partial cleavages with hydroxide; lane 4, digestion with endonuclease U2 (BRL, cuts ApN); lane 5, enzyme *B. cereus* (Pharmacia, cuts UpN or CpN); lane 6, enzyme CL3 (BRL, cuts CpN); lane 7, enzyme T1 (Pharmacia, cuts GpN), where p indicates sites of nuclease cleavage; lane 8, ribozyme reaction product (19-mer RNAs); Lane 9, partial P1 nuclease digestion (Boehringer Mannheim, no sequence specificity); lane 10, hydroxide ladder on substrate; lane 11, P1 digestion of ribozyme reaction product (all-phosphate substrate only). Sequence-specific nucleases cleave RNA to leave terminal 3′ phosphate, while alkaline hydrolysis leaves predominantly 2′-cyclic phosphates. P1 nuclease cleaves RNA to leave 3′-OH termini.

trations of ribozyme components. Therefore, k_{obs} reported for the phosphorothioate substrates (Table 1) is likely to represent k_{chem} and is directly comparable to saturating rates ($k_{cat} = k_{chem}$) of analogous phosphate substrates.

DISCUSSION

Why Create a Ribozyme from a Group II Intron? Group II introns contain active-site functionalities for catalysis of at least six distinct reactions (Augustin et al., 1990; Mörl et al., 1992; Mueller et al., 1993). And yet unlike the autocatalytic group I introns, which have a defined structural core made up of extensive phylogenetically conserved base pairings, there are no known phylogenetic covariations or pairings between the six structural domains of group II introns, and there are few conserved nucleotides (Michel et al., 1989). Thus, group II introns are important subjects for studying the fundamental basis of RNA catalysis and for exploring the relationship between structure and catalytic activity. However, the majority of group II structure/function relationships have been analyzed through self-splicing. Such

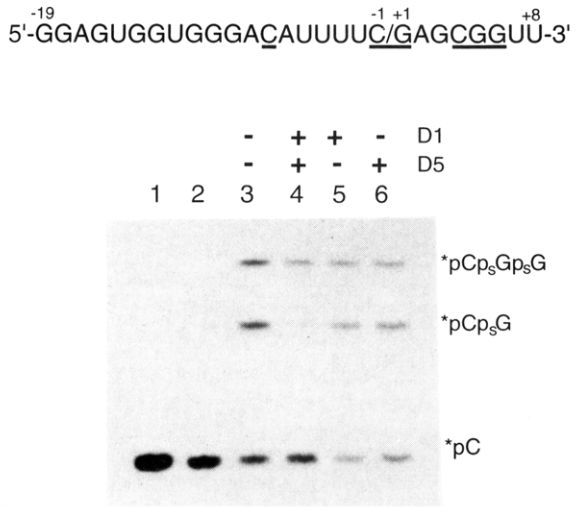

FIGURE 6: Homogeneity and specificity of cleavage at a phosphorothioate linkage. Phosphorothioate substrate was made by transcription of a DNA template as in Figure 5B, except that [α-^{32}P]CTP was included in the transcription reaction. Thus, every linkage 5′- to a G is a phosphorothioate and every phosphate 5′ to a C is doped with ^{32}P. The substrate sequence is shown at the top, and the underlined residues correspond to those species that will be 5′-^{32}P-end-labeled after complete digestion of the oligonucleotide with P1 nuclease (shown at right). Note that P1 cannot cleave Rp phosphorothioates. D1 and D5 (together with + and −) signify whether the substrate was incubated with D1 or D5 prior to P1 digestion. Lane 1: Digestion of all-phosphate substrate with P1 nuclease. Lane 2: All-phosphate substrate digested first with ribozyme, followed by P1. Lane 3: Digestion of transcribed phosphorothioate substrate with P1. Lane 4: Complete digestion of phosphorothioate substrate with ribozyme, followed by P1. Lanes 5 and 6: Digestion of phosphorothioate substrate with D1 and D5 alone, respectively, followed by P1. Any radioactivity in the middle (*pCp$_s$G) band in lane 4 corresponds to counts from the small fraction of thio-substrate (~18%) that was uncleavable by the ribozyme.

intramolecular, two-step transformations are inherently difficult to study because the observed efficiency is a function of multiple chemical steps, any of which may be complicated by structural heterogeneity or reaction reversibility. By transforming a self-splicing intron into an intermolecular ribozyme, one can dissect a single chemical reaction in which the substrate, the enzyme, and associated cofactors are physically separated. This provides experimental control over the concentrations and structures of the reaction components, which in turn allows determination of individual kinetic parameters describing the reaction mechanism.

Mechanistic Implications of the Kinetic Parameters. The agreement between single- and multiple-turnover kinetic parameters has several important implications for the overall reaction mechanism. First of all, their agreement suggests that individual reaction components (D1 and S, specifically) are conformationally homogeneous within the time scale measured in these experiments (several minutes). This is because the two methods of kinetic analysis hold opposite components rate-limiting in concentration. Under single-turnover conditions, enzyme is in excess and the concentration of substrate is vanishingly small; under multiple-turnover conditions, the converse is true. Inactive populations in either reaction component become evident when that component is present in excess (that is, rate-limiting). Consequently, if either S or D1 were in equilibrium with inactive conformational states that exchanged at a rate slower than that of chemistry, the single- and multiple-turnover values

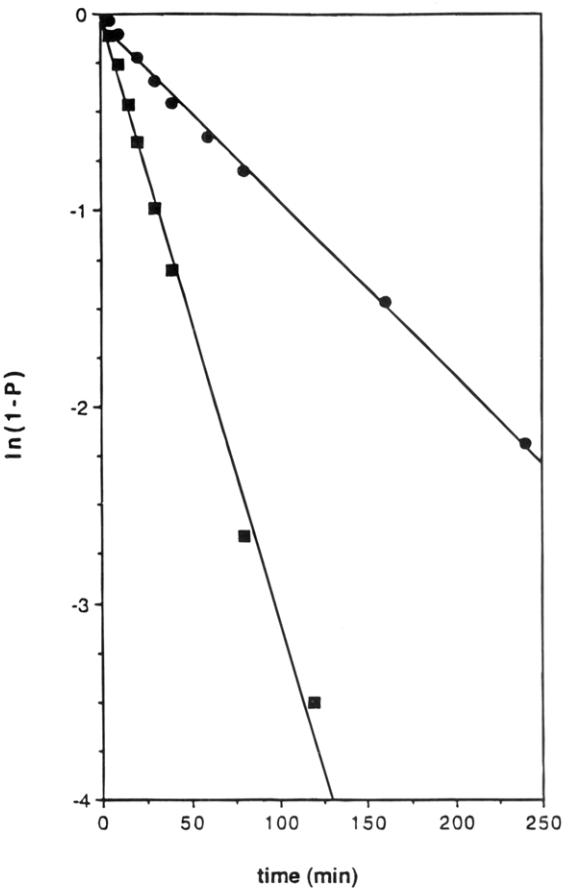

FIGURE 7: Reaction kinetics of a phosphorothioate linkage. Cleavage of the Rp phosphorothioate substrate (circles) and the transcribed all-phosphate substrate (squares) follows pseudo-first-order kinetics for more than 3 half-lives. The *y*-axis represents the natural logarithm of [1 − (fraction product)], and the *x*-axis is in minutes. Reaction conditions and saturating RNA concentrations were identical to those described in Figure 2, except [S] was 0.1 nM. Values for k_{obs} are 0.0094 and 0.032 min^{-1}, respectively (Table 1, line 4), from the average of two determinations for each plot. Errors in these values were calculated as described in Table 1. For the thio substrate, data is corrected for an empirically determined end point (at >7 half-times) of 82%. The all-phosphate substrate data is corrected for an empirically determined endpoint of 96% (at >7 half-times).

for K_m^{D1} would not match. Similarly, the K_m^{D5} reported here would not agree with the K_m^{D5} values determined through multiple- and single-turnover kinetics in a related two-part system if D5 were conformationally heterogeneous. Therefore, conformational changes intrinsic to each reaction component are unlikely to limit the rate of the reaction.

Agreement between single- and multiple-turnover parameters provides essential information about the rate-limiting step in the reaction mechanism. This follows from the fact that k_{cat} determined under single-turnover conditions (0.02−0.03 min^{-1}, in this case) reflects the rates of internal conformational change and the chemical step. This single-turnover k_{cat} is not influenced by the rate of product release because the enzyme is not allowed to turn over. A match between k_{cat} values from single- and multiple-turnover experiments indicates that, even when the ribozyme does turn over, the rate of product release is faster than that of steps that precede it. Product release (k_{off}, Scheme 1) must be faster than the minimum time necessary to measure effects on the rate of reaction ($k_{off} \geq$ (ln 2)/5 min = 0.14 min^{-1}). Further evidence for nonlimiting product release comes from

Scheme 1

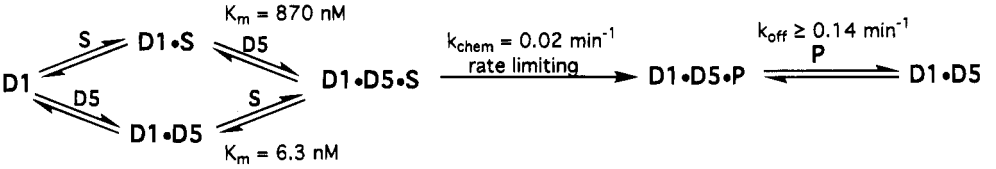

the fact that there is no initial burst in the velocity of reaction under any multiple-turnover reaction condition (data not shown).

The overall reaction is unlikely to be limited by the rate of substrate association because k_{cat}/K_m (2×10^6 M^{-1} min^{-1}) is slower than duplex annealing or binding of oligonucleotides to other ribozymes (generally $\sim 1 \times 10^8$ M^{-1} min^{-1}) (Porschke & Eigen, 1971; Herschlag & Cech, 1990; Fedor & Uhlenbeck, 1992). In addition, the saturable behavior of this ribozyme (Figure 3) suggests that a step following substrate association is rate-limiting. Apparent binding curves of k_{obs} vs [E] indicate that an E·S complex accumulates, achieving an apparent equilibrium with E and S. This happens when on-rate is fast relative to chemistry. By contrast, when association is slow, E·S reacts as fast as it forms and k_{obs} does not plateau at [E] just above K_d. For Michaelis–Menten binding behavior to result in a best fit to the data, by definition the on- and off-rates for substrate (k_1 and k_{-1}) must be fast relative to the rate of chemistry (k_2, which we call k_{cat}) (Reiner, 1959; Fersht, 1985).

Finally, comparison of kinetic parameters can help diagnose the presence of rate-limiting conformational changes within the E·S complex. Relative to K_d, a K_m determined under multiple-turnover conditions can appear smaller (tighter) in the presence of additional equilibrium constants that arise from partitioning with different conformational states (Fersht, 1985). When K_m from multiple-turnover experiments is equal to K_m from single-turnover enzyme excess experiments (which is often equivalent to K_d, as in this case), it suggests that the E·S complex is not undergoing slow internal conformational rearrangements. This appears to be true in our case because the single-turnover K_m^{D1} is approximately equal to K_d^{D1}, based on the fact that K_m^{D5} in this study is less than 2-fold different from K_d^{D5} determined directly in a previous study (Pyle & Green, 1994). Because both D5- and D1-limited single-turnover experiments result in the same k_{cat} value, if K_m^{D5} equals K_d^{D5}, then K_m^{D1} is likely to equal K_d^{D1}.

All the kinetic data are consistent with a model in which the overall rate of this reaction is limited by the chemical step. Additional support for this model is provided by the fact that phosphorothioate substitution at the cleavage site results in a small rate decrease of 2–3-fold (Table 1). The magnitude of this rate decrease, upon substitution of phosphate with phosphorothioate, has been cited as evidence for a reaction rate-limited by chemistry rather than conformational changes (Herschlag et al., 1991). This result is consistent with results from previous studies of 5′-splice-site hydrolysis by a two-piece ribozyme. In those experiments, correspondence between multiple-turnover and single-turnover kinetic parameters, together with the observations that $K_m^{D5} \approx K_d^{D5}$ and that k_{cat} was log-linear with pH, led to the hypothesis that the reaction was limited by the chemical rate of hydrolysis (Pyle & Green, 1994). The fact that D5 binding constants and k_{cat} values are within a factor of 2 for both studies suggests that the rate-limiting step in this three-part system is also chemistry. Taken together, the data are consistent with a model in which the RNA subunits in this reaction behave as independent, homogeneous components of a ternary complex that cleaves small RNA substrates at a rate limited by chemistry (Scheme 1).

Comparison with Other Ribozymes. The second-order rate constant for RNA cleavage by this ribozyme (k_{cat}/K_m^{D1} = 3.3×10^6 M^{-1} min^{-1}) is ~20× slower than that of the *Tetrahymena* ribozyme and ~40× slower than that of RNase P under single-turnover conditions. Overall rates of the latter two ribozymes are limited by substrate association under single-turnover conditions and product release under multiple-turnover conditions (Herschlag & Cech, 1990; Beebe & Fierke, 1994). A slow chemical step (~0.02–0.03 min^{-1}) appears to limit the rate of RNA hydrolysis by the group II ribozyme, and as a result, k_{cat}/K_m is lower than that of other ribozymes. Despite this slower rate, there is no reason to expect that, as a rule, ribozymes derived from group II introns will be universally slow. Different constructs of the ribozyme containing small additional substructures cleave RNA oligonucleotides at a markedly faster rate (K. Chin and A. M. Pyle, unpublished results). So far, group II intron ribozymes are unusual in that their chemical step can be observed directly, rather than by manipulation of other rate constants that limit the reaction. This feature may be useful in future studies that probe the basis for transition-state stabilization in ribozymes of this mechanistic class.

Relationship to Group II Intron Self-Splicing. The ribozyme described here behaves in a manner consistent with certain aspects of the first step of group II self-splicing (Table 2). The fact that the reaction proceeds hydrolytically, rather than through branch-point attack, does not exclude the reaction from representing the first step for several reasons. The first step of splicing can proceed by hydrolysis without preventing the second step from occurring (van der Veen et al., 1987b; Jarrell et al., 1988b). Therefore, the hydrolytic first step is a significant catalytic strategy that group II introns can exploit in order to effect splicing. Spontaneous attack of water at specific internucleotide linkages is not a favorable process in the absence of a catalyst. The uncatalyzed rate for hydrolytic cleavage of the phosphodiester linkage has been estimated to be 3×10^{-9} min^{-1} (Herschlag & Cech, 1990). Given the kinetic parameters reported here, the group II intron provides a 10^7-fold rate enhancement for hydrolytic cleavage at the 5′-splice site. Like RNase P, the group II intron contains active-site functionalities that specifically promote this reaction. Recent studies of in vitro self-splicing show that, under all reaction conditions, the first step continuously proceeds through competing hydrolytic and transesterification pathways (D. Daniels, W. J. Michels and A. M. Pyle, manuscript in preparation). Values of k_{cat} reported here are comparable to the overall rate of self-splicing under a variety of reaction conditions (D. Daniels,

W. J. Michels and A. M. Pyle, manuscript in preparation). It is well documented that the first step of self-splicing is rate-limiting in the ai5g group II intron (Jacquier & Michel, 1987; Peebles et al., 1987; Chanfreau & Jacquier, 1993). Therefore, concrete kinetic parallels link the ribozyme reported here and the overall rate of group II intron self-splicing.

The reaction reported in this study might be considered analogous to the spliced-exon-reopening, or SER, reaction promoted by group II introns in high concentrations of KCl. This is contraindicated by the fact that ligated exons are a poor substrate for the ribozyme and that our results are not unique to the KCl conditions exclusively thought to promote SER (Jarrell et al., 1988b). Efficient trans-cleavage of the small substrate occurs if KCl is replaced with any of the other monovalent salts previously reported to promote the full splicing reaction (data not shown). Although the reaction reported here is specifically inhibited by a +1C mutation like the first step of splicing, this result will not clearly distinguish our reaction from SER unless we make mutations in the first nucleotide of the 3′-exon and fail to see specific effects on the rate of SER.

In spite of apparent similarities with the first step of splicing, the reaction reported here is stereochemically more analogous to the SER reaction, which constitutes a hydrolytic reversal of the second step of splicing. It has been shown recently that the first step of splicing occurs with an apparent Sp stereospecificity (Padgett et al., 1994), while second-step reversal pathways, such as SER, proceed with Rp stereospecificity (M. Podar, P. Perlman, and R. Padgett, personal communication). On the basis of these observations, the trans-ribozyme reported here may contain an active site with attributes common to the second step of group II intron self-splicing. However, a recent study showing that the same D5 functional groups are involved in both the first and the second step implies that the two steps are not very different and that classification by splicing step may be moot (Jacquier et al., 1994).

Implications for Group II Intron Recognition of the 5′-Splice Site. The design of this ribozyme permits the first quantitative evaluation of 5′-splice-site recognition by group II introns. Both the K_m^{D1} from single-turnover experiments and the K_m from multiple-turnover experiments represent the strength of binding between oligonucleotide substrate and the D1/D5 complex. The apparent dissociation constant of 6−10 nM clearly indicates that there is strong association between the ribozyme and an oligonucleotide analogous to the 5′-splice-site. The K_m values suggest that IBS1, IBS2, and ϵ' sequences of the substrate are adequate for strong 5′-splice-site association and that additional sequences are probably unnecessary for the first step of splicing.

How much of the binding energy comes solely from D1-S interactions is not clear, although fluorescence experiments show that, in the absence of D5, D1 binds S with high affinity in the nanomolar range (Zhi-feng Qin and A. M. Pyle, unpublished results). Our results indicate that both IBS1 and IBS2 are required for recognition of the 5′-splice site by catalytic domains of the intron. An oligonucleotide composed only of IBS1 and four intronic nucleotides was not cleaved by the ribozyme. We also observe that substrates lacking the $\epsilon-\epsilon'$ interactions show significant rate decreases. Although the EBS−IBS and $\epsilon-\epsilon'$ interactions discussed so far involve base pairing, 5′-splice-site recognition by group II introns may also be mediated by tertiary interactions involving 2′-hydroxyl groups and other functionalities near the 5′-splice site. Because this is clearly the case for both group I introns and the eukaryotic spliceosome (Pyle et al., 1992; Konforti et al., 1993), investigations are underway to examine the effects of substrate backbone substituents on the reaction.

The K_m^{D5} data from this three-part system confirm that D5 interacts strongly with the other components (K_m^{D5} = 870 nM). The kinetic parameters describing the D5-dependent reaction are similar to those in a related two-part system that included D2 and D3 and covalent attachment of 5′-exon to D1 (Pyle & Green, 1994). Agreement in kinetic parameters between unimolecular, trans-D5, and three-part ribozyme constructs of the group II intron strongly suggests that covalent attachment of the 5′-exon to D1 is not required for assembly of the catalytic center and efficient cleavage at the 5′-splice site through hydrolysis.

Implications of Rp Phosphorothioate Cleavage. The 5′-splice-site specificity and mutational sensitivity of this ribozyme suggest that it mimics the first step of group II intron self-splicing. However, the ribozyme cleaves an Rp phosphorothioate linkage in the chemical step of reaction. While this implies that the reaction is related to SER, apparent Rp stereospecificity could be due to other factors as well. It was recently demonstrated that the first step of group II splicing proceeds with an overall preference for an Sp phosphorothioate diastereomer (Padgett et al., 1994). This may be due to the fact that, during the full splicing reaction, conformational changes rather than chemistry can be rate-limiting (D. Daniels, W. J. Michels, and A. M. Pyle, manuscript in preparation). Conformational changes may have stereoisomeric preferences of their own, consistent with indirect, potentially structural effects of phosphorothioates introduced into other systems (Olsen et al., 1990; Chowrira et al., 1992). However, even reactions that appear chemically limited (such as the D5-catalyzed hydrolysis of 5′-exon from domains 1−3) were observed to proceed with apparent Sp specificity (M. Podar, P. Perlman, and R. Padgett, personal communication). In these cases, although an Sp isomer was preferred, large inhibitory effects were seen for both Rp and Sp diastereomers. Therefore, the group II active site is unusual in that both nonbridging phosphate oxygens are implicated as transition-state contacts. Because our trans-ribozyme contains only a subset of group II subdomains and, potentially, a subset of transition-state interactions, it may retain contact only to the pro-Sp oxygen, resulting in apparent Rp specificity. Conversely, there may be features of 5′-splice-site addition *in-trans* that cause Rp stereospecificity to be preferred. As discussed below, major changes in the location of transition-state tertiary contacts are not required to reverse apparent stereospecificity. A recent study adds a note of caution in interpreting stereospecificity data from different studies: reaction products must be mapped to single-nucleotide resolution because phosphorothioates have been observed to promote cleavage at adjacent phosphate linkages in varieties of RNase P (Kahle et al., 1993).

Regardless of stereochemical preference, the ribozyme remains relevant to pre-mRNA splicing because snRNAs are believed to have evolved from group II domains that became separated and started to function in trans, much like our system (Sharp, 1985; Cech, 1986). It is therefore important to understand how the group II intron can be faithfully

divided into trans-ribozyme constructs. Given the modularity and minimal mechanism of our ribozyme, we may be able to build on it and identify additional structures that might be solely responsible for Sp branch formation.

Because spliceosomal processing is blocked by an Rp phosphorothioate during the first step (Maschhoff & Padgett, 1993; Moore & Sharp, 1993), one might invoke Rp cleavage by this ribozyme as evidence against a relationship between group II intron and spliceosomal processing. This would be a mistake for several reasons. Stereospecificity for a particular phosphorothioate isomer is not a quantity that is adequate for phylogenetic comparisons. First of all, it is low in information content (there are only two possible answers: Rp or Sp). But the most important reason is that minor structural differences may result in different stereospecificities by active sites that utilize the same mechanism of catalysis. Specifically, if a tertiary contact to the pro-(Rp) phosphate oxygen moves laterally by only a couple of angstroms, it will contact the pro-(Sp) oxygen instead. Given the radical structural differences between the spliceosome, group II introns, and this ribozyme, it is not unreasonable to think that such a shift might occur in the course of evolutionary time or domain fragmentation. Parallel sensitivities to mutation at the 5′-splice site provide a much more informative comparison of evolutionary relatedness between group II introns and the spliceosome. Like group II introns, it is particularly significant that +1G to +1A mutations are tolerated during the first step of spliceosomal processing, but +1C mutation inhibits reaction (Newman et al., 1985; Vijayraghavan et al., 1986; Aebi et al., 1987; Parker & Siliciano, 1993).

While it is clear from this work that the Rp diastereomer can be cleaved by the ribozyme in a reaction rate-limited by the chemical rate of catalysis, and that a 50/50 mixture of Rp and Sp isomers is only cleaved to 50%, this work does not attempt to address the absolute stereospecificity of the ribozyme in detail. Further studies on the specific chemical effects of single Rp or Sp phosphorothioates at the cleavage site, together with the effects of adding "thiophilic" metal ions, are the topic of another investigation (W. J. Michels and A. M. Pyle, manuscript in preparation).

The new group II ribozyme described here provides a quantitative description of interdomain interactions and individual rate constants for a ribozyme that cleaves an oligonucleotide resembling the 5′-splice site. This is the first case in which a group II intron has been transformed into a ribozyme shown to catalyze a single reaction on small oligonucleotide substrates. The ribozyme acts as a highly specific RNA endonuclease and consists of two independent RNA subunits that are essential for catalysis. Like other ribozymes that have been mechanistically characterized, the design of this group II ribozyme facilitates biochemical and kinetic studies required for identification of active-site residues and tertiary interactions involved in catalysis.

ACKNOWLEDGMENT

The authors wish to thank Jennifer Doudna and Olke Uhlenbeck for their insightful experimental suggestions and Thomas Cech, Daniel Herschlag, Paul Siliciano, and David Hirsh for helpful discussions. We also thank Justin Green, Kevin Chin, Melissa Moore, and Magda Konarska for their valuable comments on the manuscript. Finally, we thank Vi Chu, Danette Daniels, Kevin Chin, and Eddie Griffin for materials and permission to cite unpublished results.

REFERENCES

Aebi, M., Hornig, H., & Weissman, C. (1987) *Cell 50*, 237−246.
Altura, R., Rymond, B., Seraphin, B., & Rosbash, M. (1989) *Nucleic Acids Res. 17*, 335−354.
Augustin, S., Müller, M. W., & Schweyen, R. J. (1990) *Nature 343*, 383−386.
Beebe, J. A., & Fierke, C. A. (1994) *Biochemistry 33*, 10294−10304.
Boguski, M. S., Hieter, P. A., & Levy, C. C. (1979) *J. Biol. Chem. 255*, 2160−2163.
Cazenave, C., & Uhlenbeck, O. C. (1994) *Proc. Natl. Acad. Sci. U.S.A. 91*, 6972−6976.
Cech, T. R. (1986) *Cell 44*, 207−210.
Chanfreau, G., & Jacquier, A. (1993) *EMBO J. 12*, 5173−5180.
Chanfreau, G., & Jacquier, A. (1994) *Science 266*, 1383−1387.
Chowrira, B. M., & Burke, J. M. (1992) *Nucleic Acids Res. 20*, 2835−2840.
Donis-Keller, H., Maxam, A. M., & Gilbert, W. (1977) *Nucleic Acids Res. 4*, 2527−2538.
Fedor, M. J., & Uhlenbeck, O. C. (1992) *Biochemistry 31*, 12042−12054.
Ferat, J.-L., & Michel, F. (1993) *Nature 364*, 358−361.
Ferat, J.-L., Le Gouar, M., & Michel, F. (1994) *C. R. Acad. Sci., Ser. 3 317*, 141−148.
Fersht, A. (1985) *Enzyme structure and mechanism*, pp 101−111, W. H. Freeman, New York.
Franzen, J. S., Zhang, M., & Peebles, C. L. (1993) *Nucleic Acids Res. 21*, 627−634.
Griffiths, A., Potter, B., & Eperon, I. (1987) *Nucleic Acids Res. 15*, 4145−4162.
Guerrier-Takada, C., Gardiner, K., Marsh, T., Pace, N., & Altman, S. (1983) *Cell 35*, 849−857.
Herschlag, D., & Cech, T. R. (1990) *Biochemistry 29*, 10159−10171.
Herschlag, D., Piccirilli, J. A., & Cech, T. R. (1991) *Biochemistry 30*, 4844−4854.
Jacquier, A., & Rosbash, M. (1986) *Science 234*, 1099−1104.
Jacquier, A., & Michel, F. (1987) *Cell 50*, 17−29.
Jacquier, A., & Michel, F. (1990) *J. Mol. Biol. 213*, 437−447.
Jarrell, K. A., Dietrich, R. C., & Perlman, P. S. (1988a) *Mol. Cell. Biol. 8*, 2361−2366.
Jarrell, K. A., Peebles, C. L., Dietrich, R. C., Romiti, S. L., & Perlman, P. S. (1988b) *J. Biol. Chem. 263*, 3432−3439.
Kahle, D., Küst, B., & Krupp, G. (1993) *Biochimie 75*, 955−962.
Koch, J. L., Boulanger, S. C., Dib-Hajj, S. D., Hebbar, S. K., & Perlman, P. S. (1992) *Mol. Cell. Biol. 12*, 1950−1958.
Konforti, B. B., Koziolkiewicz, M. J., & Konarska, M. M. (1993) *Cell 75*, 863−873.
Kruger, K., Grabowski, P. J., Zaug, A. J., Sands, J., Gottschling, D. E., & Cech, T. R. (1982) *Cell 31*, 147−157.
Kück, U., Godehardt, I., & Schmidt, U. (1990) *Nucleic Acids Res. 18*, 2691−2697.
Maschhoff, K. L., & Padgett, R. A. (1993) *Nucleic Acids Res. 21*, 5456−5462.
Michel, F., & Dujon, B. (1983) *EMBO J. 2*, 33−38.
Michel, F., Umesono, K., & Ozeki, H. (1989) *Gene 82*, 5−30.
Milligan, J. F., & Uhlenbeck, O. C. (1989) *Methods Enzymol. 180*, 51−62.
Moore, M. J., & Sharp, P. A. (1993) *Nature 365*, 364−368.
Mörl, M., Niemer, I., & Schmelzer, C. (1992) *Cell 70*, 803−810.
Mueller, M. W., Hetzer, M., & Schweyen, R. J. (1993) *Nature 261*, 1035−1038.
Muller, M. W., Schweyen, R. J., & Schmelzer, C. (1988) *Nucleic Acids Res. 16*, 7383−7395.
Newman, A. J., Lin, R.-J., Cheng, S.-C., & Abelson, J. (1985) *Cell 42*, 335−344.
Olsen, D. B., Kotzorek, G., Sayers, J. R., & Eckstein, F. (1990) *J. Biol. Chem. 265*, 14389−14394.
Padgett, R. A., Podar, M., Boulanger, S. C., & Perlman, P. S. (1994) *Science 266*, 1685−1688.
Parker, R., & Siliciano, P. G. (1993) *Nature 361*, 660−662.

Peebles, C. L., Perlman, P. S., Mecklenburg, K. L., Petrillo, M. L., Tabor, J. H., Jarrell, K. A., & Cheng, H.-L. (1986) *Cell 44*, 213–223.

Peebles, C. L., Belcher, S. M., Zhang, M., Dietrich, R. C., & Perlman, P. C. (1993) *J. Biol. Chem. 268*, 11929–11938.

Peebles, C. L., Benatan, E. J., Jarrell, K. A., & Perlman, P. S. (1987) *Cold Spring Harbor Symp. Quant. Biol. 52*, 223–232.

Porschke, D., & Eigen, M. (1971) *J. Mol. Biol. 62*, 361–381.

Potter, B. V. L., Connolly, B. A., & Eckstein, F. (1983) *Biochemistry 22*, 1369–1376.

Pyle, A. M., & Green, J. B. (1994) *Biochemistry 33*, 2716–2725.

Pyle, A. M., Murphy, F. L., & Cech, T. R. (1992) *Nature 358*, 123–128.

Reiner, J. M. (1959) *Behavior of Enzyme Systems*, pp 54–63, Burgess Publishing Company, Minneapolis.

Scaringe, S. A., Francklyn, C., & Usman, N. (1990) *Nucleic Acids Res. 18*, 5433–5441.

Schatz, D., Leberman, R., & Eckstein, F. (1991) *Proc. Natl. Acad. Sci. U.S.A. 88*, 6132–6136.

Schmelzer, C., & Schweyen, R. J. (1986) *Cell 46*, 557–565.

Schmidt, U., Kosack, M., & Stahl, U. (1987) *Curr. Genet. 12*, 291–295.

Schmidt, U., Riederer, B., Morl, M., Schmelzer, C., & Stahl, U. (1990) *EMBO J. 9*, 2289–2298.

Sharp, P. A. (1985) *Cell 42*, 397–400.

Slim, G., & Gait, M. J. (1991) *Nucleic Acids Res. 19*, 1183–1188.

Suchy, M., & Schmelzer, C. (1991) *J. Mol. Biol. 222*, 179–187.

van der Veen, R., Arnberg, A. C., van der Horst, G., Bonen, L., Tabak, H. F., & Grivell, L. A. (1986) *Cell 44*, 225–234.

van der Veen, R., Arnberg, A. C., & Grivell, L. A. (1987a) *EMBO J. 6*, 1079–1084.

van der Veen, R., Kwakman, J. H. J. M., & Grivell, L. A. (1987b) *EMBO J. 6*, 3827–3831.

Vijayraghavan, U., Parker, R., Tamm, J., Iimura, Y., Rossi, J., Abelson, J., & Guthrie, C. (1986) *EMBO J. 5*, 1683–1695.

Wallasch, C., Mörl, M., Niemer, I., & Schmelzer, C. (1991) *Nucleic Acids Res. 19*, 3307–3314.

Zaug, A. J., & Cech, T. R. (1986) *Science 231*, 470–475.

Zaug, A. J., Been, M. D., & Cech, T. R. (1986) *Science 324*, 429–433.

BI942229V